MPS/Int. RF 64 - 2
2.3.1964

ON THE CALIBRATION OF THE INTENSITY PU-STATION

Summary

This report gives the methods by which the intensity measurement with an electrostatic pick-up electrode has been calibrated.

Two means of calibration are described and the result of the calibration is checked by comparing digital intensity indication (which is derived from the electrostatic pick-up arrangement) with the readings of the current transformer (Hereward transformer).

Index

1. Introduction

For the intensity measurement of the proton beam in the PS an electrode is used which encircles the proton beam.

The capacitance of this electrode to earth is charged by influence due to the charge in the proton beam.

As this beam is bunched, the voltage across this capacity has the form of a pulse train. If we call the amplitude of the fundamental of this pulse train $\hat{U}_e$, then the following relation exists between the number of circulating protons and this voltage :

$$A_p = K \cdot \hat{U}_e \qquad (1)$$

where K is the calibration constant and A_p the number of protons.

The calibration of the PU station consists in the evaluation of K. This K is a function of the geometry of the PU station and the charge distribution in the accelerator, as well as of the loading of the electrode by the input circuit of the cathode follower.

While the geometry of the PU station of course remains constant, as does the load, the charge distribution around the ring does not, due to bunch formation during the initial period of the acceleration. As this charge distribution can be considered to be rather constant and defined at energies above transition, the intensity measurement is carried out in the energy range over 5 GeV.

The input circuit of the cathode-follower consists of capacitances and resistances that safeguard the circuit against overloading. The influence of the capacitive component of the circuit is taken directly into account in the calibration of the PU station while the influence of the resistive component is considered separately in section 6.

Since the calibration constant K from equation (1) must be evaluated in the laboratory, the proton beam must be simulated.

It is rather simple to simulate the first harmonic of the beam signal, moreover it is possible to simulate a perfectly debunched proton beam. Both

ways of beam simulation have been used and the resulting calibration methods are described in section 2 and 3.

Before proceeding to these descriptions, a brief summary of the fundamentals applicable to both calibration methods will be given below.

The voltage across the electrode capacitance can be written as :

$$U_e = \frac{Q}{C} \tag{2}$$

In our case the Q represents the charge which has been induced on the electrode by the proton beam and the C represents the total capacitance between electrode and earth. For an eletrode with additional capacitive loading the value of C is :

$$C = C_e + C_z \tag{3}$$

C_e = electrode capacity
C_z = sum of add. capacity

Assuming for the moment that the number of protons is constant, and with that the induced charge Q, equations (2) and (3) can be written as :

$$\frac{1}{U_e} = \frac{C_e + C_z}{Q} \tag{4}$$

This shows that $\frac{1}{U_e}$ is a linear function of C_z and that the ordinate is cut at $C_z = - C_e$.

After finding this point the slope of the function has to be evaluated in order to complete the calibration .

2. Calibration on the basis of coaxial transmission line theory

The fundamental of the beam signal is simulated in a reflexion-free coaxial transmission line of which the PU station is an integral part.

This chapter is devided into the following parts :

a) fundamental of the proton beam at 5 GeV and avove,

b) charge density on a coaxial line,

c) the coaxial line,

d) measurement results.

a) Fundamental of the proton beam at 5 GeV and above

The connection between the actual charge distribution in the accelerator and its fundamental at high energies is shown in fig. 1, where

q_p = amplitude of everage charge

q_f = peak value of fundamental

The relation :

$$2\, q_p = q_f \tag{5}$$

is valid on condition that $\varphi \ll \lambda$ (ref. Konopasek).

The number of protons in the accelerator follows from :

$$A_p = \frac{\text{total charge}}{\text{elementary charge}} \tag{7}$$

which we write as :

$$A_p = q_p \cdot \frac{L}{e} \tag{8}$$

where $L = 628$ m = circumference of accelerator,

$e = 1{,}6 \cdot 10^{-19}$ coulomb = elementary charge.

From (5) and (8) follows :

$$q_f = 2 \frac{A_p e}{L} \tag{9}$$

Now, in order to simulate A_p protons, we have to generate on the coaxial line a charge density as given in equation (9).

b) Charge density on a coaxial line

Independent of the place of measurement on a coaxial line the charge density is given by:

$$q_{f\ell} = \frac{\hat{U}_o}{c\,Z} \tag{10}$$

if the coaxial line is without discontinuities and terminated into its characteristic impedance Z.

$\hat{U}_o$ = Voltage on the central conductor

c = velocity of light.

The velocity of charge on a coaxial line is (with vacuum or air as dielectricum) near enough the velocity of light. Ohmic and dielectric losses can be neglected, if the line is short and has air dielectric.

In equation (10) we may replace the value of $q_{f\ell}$ by the value q_f of equation (9) if the protons in the PS have the velocity of light. This is given with good approximation at high energies.

So we get from (9) and (10) :

$$A_p = \frac{\hat{U}_o \cdot L}{2\,ecZ} \tag{11}$$

If we call

$$\frac{\hat{U}_o}{\hat{U}_e} = K_1$$

then (11) can be written as

$$A_p = \frac{K_1 L}{2 Zec} \cdot \hat{U}_e \qquad (11a)$$

where $\hat{U}_e$ = voltage on the electrode.
If we collect all constants in a factor

$$K = \frac{K_1 L}{2 ecZ}$$

then we can write for (11a)

$$A_p = K \hat{U}_e \qquad (11b)$$

c) <u>The coaxial line</u>

The outer conductor of the coaxial line was constructed from the complete PU station with an additional 4 m of standard vacuum chamber. The centre conductor was made of a wire of 2 mm diameter inside the 4 m of vacuum chamber and with some additional diameter modifications inside the PU station.

These modifications were necessary to maintain the same characteristic impedance inside the PU station as in the vacuum chamber.

The diameter of the centre conductor in the space inside the PU station tank which is free from influence of the PU electrodes is a function of the diameter of the tank and the characteristic impedance. However, in the spaces where the PU electrodes have influence, the diameter depends also on the additional capacities C_{z1} or C_{z2}.

In fig. 2 the coaxial line is shown schematically. In the space where no influence of the electrode is present, the diameter of the centre conductor is :

$$d = D\, e^{-Z/60} \tag{12}$$

In the space where the electrode has influence this diameter is :

$$d^*_{1,2} = D^*\, e\, \exp\left(\frac{C^*_{eo} \ln D/D^*}{C^*_e + C_{z1,2}} - Z/60\right) \tag{13}$$

(For evaluation of (13) see appendix 1)

The meaning of the capacitances is :

C^*_{eo} is the capacitance of the electrode without longitudinal electrical field. $C^*_{eo} = 20$ pF.

C^*_e is the capacitance of the electrode with longitudinal electrical field.

As the exact value of C^*_e is not known, we make the calibration measurements with two values which are considered the limits of C^*_e :

$$C^*_{e\,1} = C^*_{eo} = 20 \text{ pF}$$

$$C^*_{e\,2} = C_e = 32{,}3 \text{ pF (measured value)}$$

C_z is the externally added capacitance.

C_c is the capacity between the two electrodes (calculations and measurements, see chapter 5)

d) Measurement Results

The characteristic impedance of that part of the coaxial line which consisted of the vacuum chamber and the 2mm centre conductor, had a measured value of

$$Z = 224 \text{ ohms} \qquad (14)$$

The value of the characteristic impedance in the PU station was therefore designed to have the same value.

The diameters of the centre conductor in the space where the electrode has influence were chosen as :

$$d^*_1 = 6{,}3 \text{ mm}$$

$$d^*_2 = 4 \text{ mm}$$

The loading capacitances for these two diameters were computed with equation (13) where capacitance C^*_e was taken as 20 pF and 32,3 pF as min. and max. values for each of the two diameters.

$$C_{z11} = 12 \text{ pF}; \qquad C_{z12} = 0 \text{ pF}$$

$$C_{z21} = 328 \text{ pF}; \qquad C_{z22} = 316 \text{ pF}$$

As it was not possible to measure the voltage on the electrode with $C_{z12} = 0$ pF (the capacitance of the probe was already 2,5 pF) we had to measure some points in the neighbourhood of $C_z = 0$ pF in order to find the

desired value by extrapolation.

The measurement results are tabulated in Table 1. The voltage on the centre conductor was U_o = 2,42 V_{eff} = const. This voltage according to equation (11) corresponds to the number of protons $A_p = 10^{11}$ protons.

$U_o\ 10^{11}$ = 2,42 V_{eff}						
$C^*_{e1,2}$ (pF)	d^* (mm)	C_z (pF)	U_o (V_{eff})	U_e (mV_{eff})	$U_{e10^{11}}$ (mV_{eff})	$\frac{1}{U_{e10^{11}}}$ ($\frac{1}{mV_{eff}}$)
20	4	328	10	145	35,1	28,5
20	6,3	12	10	1080	261,5	3,83
32,3	4	316	10	150	36,3	27,5
32,3	6,3	28,5	10	910	220	4,54
32,3	6,3	18,4	10	1020	247	4,05
32,3	6,3	12	10	1170	283	3,53
32,3	6,3	6,4	10	1320	320	3,13
32,3	6,3	2,5	10	1370	331,5	3,02

Table 1

In fig. 3 the measurement results are plotted with $\frac{1}{U_{o\ eff}}$ as ordinate and C_z as abscissa. We see that both pairs of points produce practically the same straight line. But this could be a coincidence.

U_e was measured with a high impedance voltmeter making only a capacitive extra loading of 2,5 pF. The overall calibration also needs to take account of

the gain of the cathode-follower (including its input circuit).

In order to show, that in drawing 3 one should find a straight line, we used the formula (4)

$$\frac{1}{U_e} = \frac{C_e + C_z}{Q}$$

This assumes that Q is constant along the line. This is not precisely true for the following reason : we attempted to make Q constant by calculating a suitable C_z for each d^*, but this calculation needs C_e^*, which is not known. So we had to use an upper or lower limit estimate. So, in fact, C_z and d^* do not precisely have values correctly related to make Q constant. But we think this difficulty produces only a very small error.

The slope of the calibration curve is from fig. 3 :

$$\operatorname{tg} \alpha_1 = 0{,}0784 \cdot 10^{12} \left(\frac{1}{FV_{eff}}\right) \qquad (15)$$

With this the factor K from equation (1) is

$$K = \operatorname{tg} \alpha_1 \cdot 10^{11} (C_{e1} + C_z) \qquad (16)$$

so that we find as relation between A_p and U_e :

$$A_p = 78{,}4 \cdot 10^{20} (C_{e1} + C_z) U_{eeff} \qquad (17)$$

The calibration curve cuts the ordinate (fig. 3) in the point

$$- C_{e1} = - 36 \text{ pF} .$$

3. Calibration with a charged rod

a) Method

In accordance with what we have said in the introduction, the debunched proton beam will now be simulated by a charged rod. The charge is uniformly distributed along a discrete part (ℓ) of the rod length.

ℓ was, of course, made longer than the space in which the influence of the electrode is present.

The charge Q_i influenced on the electrode, was collected in a defined capacitance C_{M1} and evaluated by means of a voltage measurement.

The evenness of the charge distribution was checked by a special electrode (K), see fig. 4.

To determine Q_g, the total charge on ℓ, the rod was pushed into a conducting cylinder, which was longer than ℓ. Thus on the cylinder the same number of elementary charges was influenced as the length ℓ of the rod was carrying.

The total of the influenced charge was again collected in a defined capacitance C_{M2} and evaluated by means of a voltage measurement.

It goes without saying that the cylinder was free from earth.

The charge per unit of length is :

$$q_s = \frac{Q_g}{\ell} = \frac{U_g (C_{M2} + C_R)}{\ell} \qquad (18)$$

where

Q_g = total charge

ℓ = length of charged rod

U_g = Voltage on C_{M2}

C_{M2} = standard capacitance

C_R = capacity of the cylinder to earth $\approx$ 90 pF

The equivalent charge in the accelerator can be written as (see equation (8)):

$$q_p = \frac{A_p e}{L} \tag{19}$$

The ration of q_s and q_p is :

$$\frac{q_s}{q_p} = \frac{U_i (C_{M1} + C_e)}{U_e (C_e + C_z)} \tag{20}$$

where

U_i = electrode voltage as influenced by rod charge

C_{M1} = standard capacitance

U_e = electrode voltage as influenced by debunched proton beam

Substitution of (18) in (20) yields for U_e :

$$U_e = \frac{U_i (C_{M1} + C_e)\, \ell}{U_g (C_e + C_z)(C_{M2} + C_R)} \cdot q_p \tag{21}$$

As we have chosen $C_{M1} \gg C_e$ and $C_{M2} \gg C_R$ and while $C_{M1} = C_{M2} = 0{,}2$ /uF, equation (20) becomes :

$$U_e \approx \frac{\ell}{C_e + C_z} \cdot \frac{U_i}{U_g} q_p \tag{22}$$

So far we have only considered static conditions. The relation between the fundamental of bunched proton beam and debunched proton beam is given by

$$\frac{q_p}{q_f} = \frac{U_e}{\hat{U}_e} \qquad (23)$$

With equations (5), (19), and (23) we get for the number of protons :

$$A_p = \frac{L\,(C_e + C_z)}{2\,\ell \cdot e} \cdot \frac{U_g}{U_i} \cdot \hat{U}_e \qquad (24)$$

Again we call $\frac{U_g}{U_i} = K_2$, and $K = \frac{K_2\, L\,(C_e + C_z)}{2\,\ell\, e}$.

According to the introduction we get :

$$A_p = K\,\hat{U}_e \qquad (25)$$

b) Measuring equipment

The arrangement is shown in fig. 4.

The rod was of PVC material, obtained from the SB electricity shop and was charged simply by rubbing it with shammy-leather.

With the control electrode (k) the continuity of the charge was checked. Voltage variations up to 15 % of U_{Kmax} were tolerated. A cord was used as a means of transport. The voltage was measured with a Keithley-Electrometer Model 210.

The time constant of the measurement was practically determined by the resistivity of the supporting bars of the electrode (porcelain). The input resistance of the electrometer was of no practical importance. Before the measurements were made, it was necessary to dry the whole arrangement with hot air. In this way, a time constant of greater than 1 hour was achieved.

Fig. 4 shows a simplified sketch of the PU station. For the actual measurement the complete PU station was used (see fig. 2, without central conductor). The second electrode was connected to earth. It remained to be seen whether the surface conductivity of the rod was sufficiently small so that no charge displacement occurred during the measurement.

This has been shown in the following way (see fig. 5):

The rod was placed in a metallic cylinder A which was connected to earth via capacitor C. The part of the rod which is shaded in fig. 5 was previously charged. The voltage across the capacitor C was U.

Next, a second metallic cylinder B, which narrowly encircled the rod without however touching it, was brought into cylinder A. As the cylinder B had a galvanic connection with earth the voltage across the capacitor C disappeared.

Now, when cylinder B was pulled out of cylinder A at a speed of about 0.1 cm/sec and brought back into its original position outside the cylinder A, the voltage across C was again at its original value.

We believe that, from this and similar experiments, we may assume that the surface conductivity of the rod was sufficiently small.

c) Result of measurements

We have performed 20 independent measurements which resulted in an average value for K_2 of :

$$K_{2m} = 2,12 \qquad (26)$$

The spread was smaller than 6% of K_{2m} and the voltages of U_i and U_g were in the order of 1 Volt.

With equations (24), (25) and (26) we may write the calibrations curve as :

$$\frac{1}{U_{e_{eff}}} = \frac{K}{A_p} = \frac{K_{2m} \cdot L}{\sqrt{2}\, \ell_e\, A_p} (C_e + C_z) = \operatorname{tg} \alpha_2 \, (C_e + C_z) \qquad (27)$$

where

$$\operatorname{tg} \alpha_2 = \frac{K_{2m}\, L}{\sqrt{2}\, \ell_e A_p} \qquad (28)$$

A factor $\sqrt{2}$ appears in the denominator if U_e is written as an effective voltage. If in (28) we take $A_p = 10^{11}$ protons, $L = 628$ m, $\ell = 70$ cm, and $e = 1{,}6 \cdot 10^{-19}$ coulombs we get :

$$\operatorname{tg} \alpha_2 = 0{,}0844 \cdot 10^{12} \left[\frac{1}{VF}\right] \qquad (29)$$

With this tangent we can draw the calibration curve as we have done in fig. 6. The voltage U_e is of course the voltage on the electrode, not at the output of the cathode-follower.

4. Remarks on the two methods

The two measurement methods should be regarded as complementary. While in the first method (coaxial line) we measured the calibration line directly by measuring some points of it and computed the slope of the curve from the drawing, in the second method (charged rod) we in fact measured the slope of the line and we constructed this line afterwards.

Comparing the results of the two methods we find some differences both in the slope of the calibration curves and in the effective capacity of the electrode.

In fig. 7 we give the differences of the two curves in % of the average of these curves as a function of C_z .

It is of course very difficult to decide which of the two curves is the more exact. Perhaps we may regard a line between the two as the most exact.

5. The influence of the coupling capacitance C_c

The capacitance between the two electrodes in the two halves of the station is not completely negligible. In the case of the proton beam in the PS we can distinguish 3 possibilities :

1. The two halves of the station have the same loading C_z, so the electrodes pick up the same voltage (neglecting the small phase difference between them). In this case the capacitance between them has no voltage across it and so no effect.

2. We work with one electrode, the other is earthed or has a much larger C_z than the one we are using. The capacitance between them, or most of it, acts as extra capacity on the one that we are using, and we obtain less signal than in case (1).

3. We work with one electrode, the other has a smaller C_z and goes to a higher voltage. The capacitance makes the electrode we are using read higher than in case (1).

The combination of cases (2) and (3) very nearly describe the actual conditions. To calculate the effect of C_c we may regard the problem as follows (see fig. 8) :

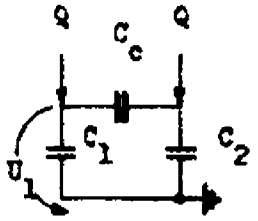

Fig. 8

We found the relation :

$$U_1 = Q \frac{2C_c + C_2}{C_1C_2 + C_1C_c + C_2C_c} \qquad (30)$$

We measured $C_c = 1{,}3$ pF .

The capacitances of the electrodes with their actual total loading are ≈ 52 pF and ≈ 252 pF. With this and equation (30) we get for case (2) a reduction of the signal in the order of about 1,6 %.

For case (3) we get an increase of about 2 %. To examine our calculations we made a very simple measurement with the PS :

We connected the electrode which has the big loading capacitance with the intentity reading system and the other electrode was left under normal working conditions. Then we noted down the reading of the pick-up electrode and the reading of the current transformer during 20 machine pulses. After that the electrode which has normally the small loading capacitance was connected to earth and we made the readings again during 20 machine pulses. We found a reduction of the pick-up signal of about 1.85 %. With equation (30) we found for this case a reduction of about 2.6 %. It seems that C_c is a little smaller than the value we have measured.

This effect of C_c may be taken into account for the measurement results according to method 2 (charged rod). We remember that the second electrode was earthed during these measurements. So we have to decrease the value of $tg\ \alpha_2$ (see equation 29) by about 1,85 %.

It seems difficult to say how to take account of the effect of C_c in the result of the measurements according to method 1 (coaxial line).

6. The influence of a resistance between electrode and additional capacitance

As was mentioned before, a resistance is connected between the electrode capacity and the additional capacitance in order to prevent overloading of the cathode-follower.

The capacitance which we have so far called C_z is split into two parts by this resistance, one part is C_{zo}, formed by the capacity between electrode and test probes and vacuum-tight connectors, the other part is the added capacitance which for reasons of simplicity we call again C_z. So

$$C_e' = C_e + C_{zo}$$

where $C_{zo} \approx 8$ pF .

The influence of the resistance was measured with the PS. The measurement is rather simple as we have two separate PU-electrodes at our disposal. One was used for the measurement itself while on the other the fundamental of the signal as a function of R and C_z was measured. After normalization of the measured fundamental to intensity we get the attenuation factor b dependent on the values of R and C_z. Fig. 9 shows the resulting curves.

With fig. 9 and the results of chapter 2 or 3 we can construct the final calibration curves. This was done in fig. 10, basing on the result of chapter 3 (charged rod) and neglecting the effect of the capacitance C_c

between the two electrodes. In fig. 10 U_e means the input voltage of the cathode-follower measured in V_{eff}.

7. Comparison of the intensity indications as obtained by the current transformer and the PU arrangement

The intensity station was calibrated according to fig. 10 for $A_p = 5.10^{11}$ protons. The actual values for R and C_z were :

$$R = 330 \text{ ohms}$$

$$C_z = 200 \text{ pF}$$

while

$$C_e' = 40 \text{ pF}$$

Any change in these values of course results in a change in the calibration factor. One should pay attention to the fact that any change in C_e', e.g. a change in test probe sensitivity etc., may result in a considerable change in the calibration factor.

The intensity reading of the calibrated station was compared with the reading of the Hereward transformer. This comparison was made in three intensity ranges (in total over 2500 machine pulses).

The result is shown in fig. 11. The thick line is the average and the spread is show. It should be pointed out here that in the low intensity range the printer printed one digit less than in the other two ranges which means that spread and also average could not be accurately drawn.

In the higher intensity ranges the current transformer indicated a current higher than that given by the PU station (see fig. 11). We supposed that some sort of overloading occurs between the input of the cathode-follower and the digital reading. A plot of cathode-follower input voltages versus digital read-outs also indicates this tendency (see fig. 12).

APPENDIX 1

In this appendix some additional considerations on the structure of the coaxial line are given. The total measuring set-up is shown in fig. 13 (scale 1:2,5).

a) Centre conductor

For the calculation of the centre conductor, the procedure is the following :

The load capacitance C_z is considered to be compensated by a change in tank diameter in such a way that between electrode and tank the capacitance equals $C^*_o + C_z$. Thus a fictional tank-diameter D_f is obtained for the space where the electrode is of influence. With this fictional value for D_f and the already obtained characteristic impedance Z, the diameter of the centre conductor is calculated.

According to this approach we can write :

$$C^*_{eo} + \Delta C^*_e + C_z = \frac{2\pi \varepsilon_o a}{\ln D_f/D^*} \qquad (1)$$

ΔC^*_e is any extra capacitance that comes from the longitudinal electric field in the PU station. From (1) follows :

$$D_f = D^* e \exp \frac{2\pi \varepsilon_o a}{C^*_{eo} + \Delta C^*_e + C_z} \qquad (2)$$

with

$$Z = 60 \ln \frac{D_f}{D^*} \qquad (3)$$

we obtain

$$d^* = D^* \, e \, \exp\left(\frac{2\pi \, \varepsilon_0 \, a}{C^*_{eo} + \Delta C^*_e + C_z} - Z/60\right) \tag{4}$$

with

$$C_{eo} = \frac{2\pi\varepsilon_0 \, a}{\ln D/D^*}$$

or

$$2\pi \, \varepsilon_0 \, a = C^*_{eo} \ln D/D^*$$

and

$$C_{eo} + \Delta C^*_e = C^*_e$$

we get for equation (4):

$$d^* = D^* \, e \, \exp\left(\frac{C^*_{eo} \ln D/D^*}{C^*_e + C_z} - Z/60\right) \tag{5}$$

In order to obtain an idea of the characteristic impedance of the PU electrode with the 4 m of the vacuum chamber, the generator voltage U_o (fig. 13) was kept constant and U_z was measured as a function of the frequency.

The frequency was changed between 10 and 20 MHz. In this frequency band a minimum for $\frac{U_z}{U_o}$ was found:

$$\frac{U_z}{U_o} = 0.972$$

The line, constructed from the vacuum chamber directly terminated in Z, showed no detectable mismatch in the same frequency band.

In this measurement, the total length of the vacuum chamber was 4,5 m (i.e., the complete measurement set-up without the PU station).

APPENDIX 2

For completion the cathode-follower circuit is given as it was designed and measured by P. Gottfeldt.

The circuit of the cathode follower is shown in fig.14.

The design is simple and the principal difficulty encountered was the avoidance of high frequency oscillations due to the 200 pF at the grid. This necissitated the use of a fairly high value grid stopper.

The D.C. operating conditions and the RF gain are indicated below:

D.C. operating conditions = I_a = 28 mA; U_c = 2.3 V (with 75 ohms termination)

RF gain (9.55 Mc/s) :

From grid to cathode gain = 0,7, including
330 ohms resistor gain = 0,16.

ACKNOWLEDGMENTS

The author wishes to thank H.G. Hereward for his support and the interest which he has shown in this work.

He is also very grateful to H. Fischer, K. Gase et P. Gottfeldt for many helpful discussions. He is further indebted to K. Köhler and the operating staff of the Main Control Room for their assistance during the measurements necessary for this report.

R.K. Kaiser

Distribution : (open)

MPS Scientific and Technical Staff
RF Group

REFERENCES

1. F. Kanopasek : Proposed Beam Current Measuring System
(PS/Int. MG 60-16, of 25-2-1960)

2. F. Konopasek : Probable Accuracy of Beam Current Measuring Equipment
(PS/Int. MG 60-37, of 4-5-1960)

3. H. Fischer : Beam Intensity Measurement
(PS/Int. MG/RF 60-6, of 27-5-1960)

4. H. Fischer, R.K. Kaiser : Calibration of PU station 57 with coaxial wire
(MPS/RF memorandum of 30-3-1961)

5. Jack B. Sharp : The Induction Type Beam Monitor for the P.S.
(MPS/Int. CO 62-15, of 6-12-1962)

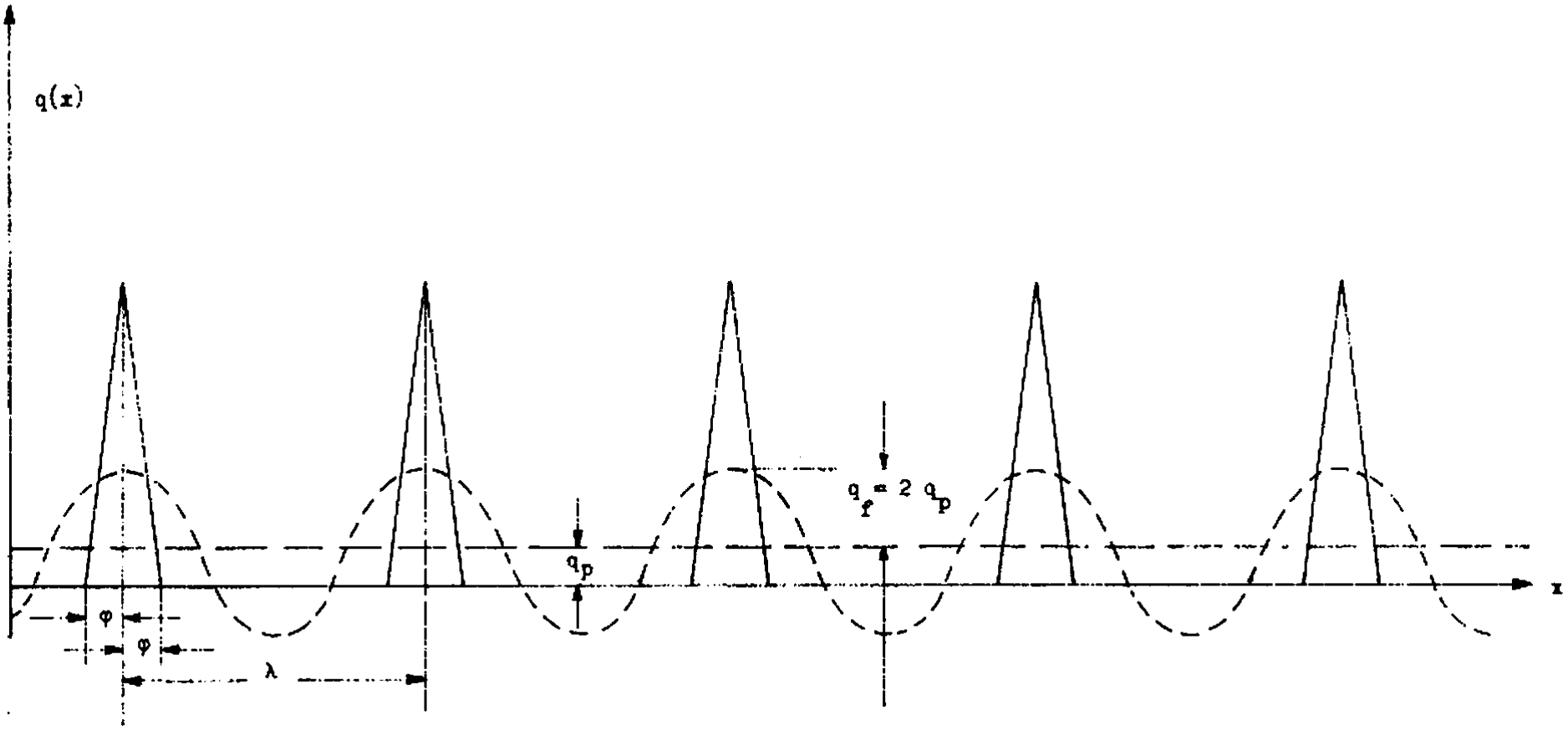

Fig. 1

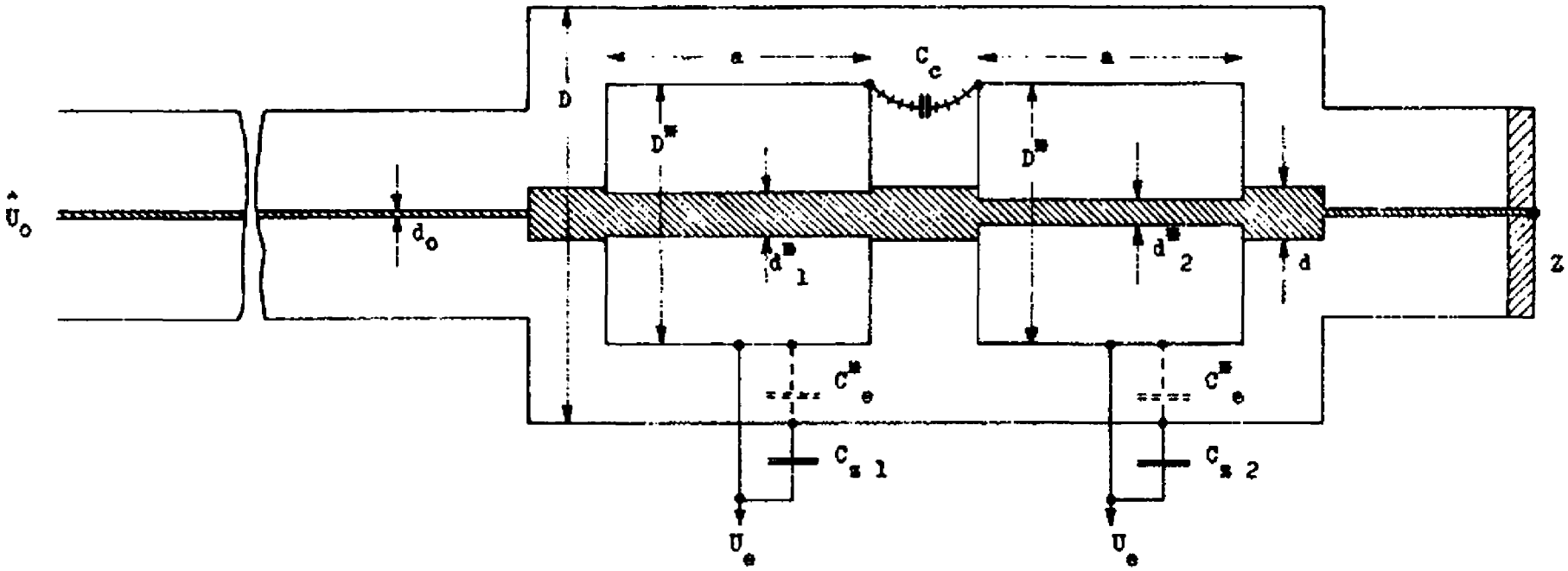

Fig. 2

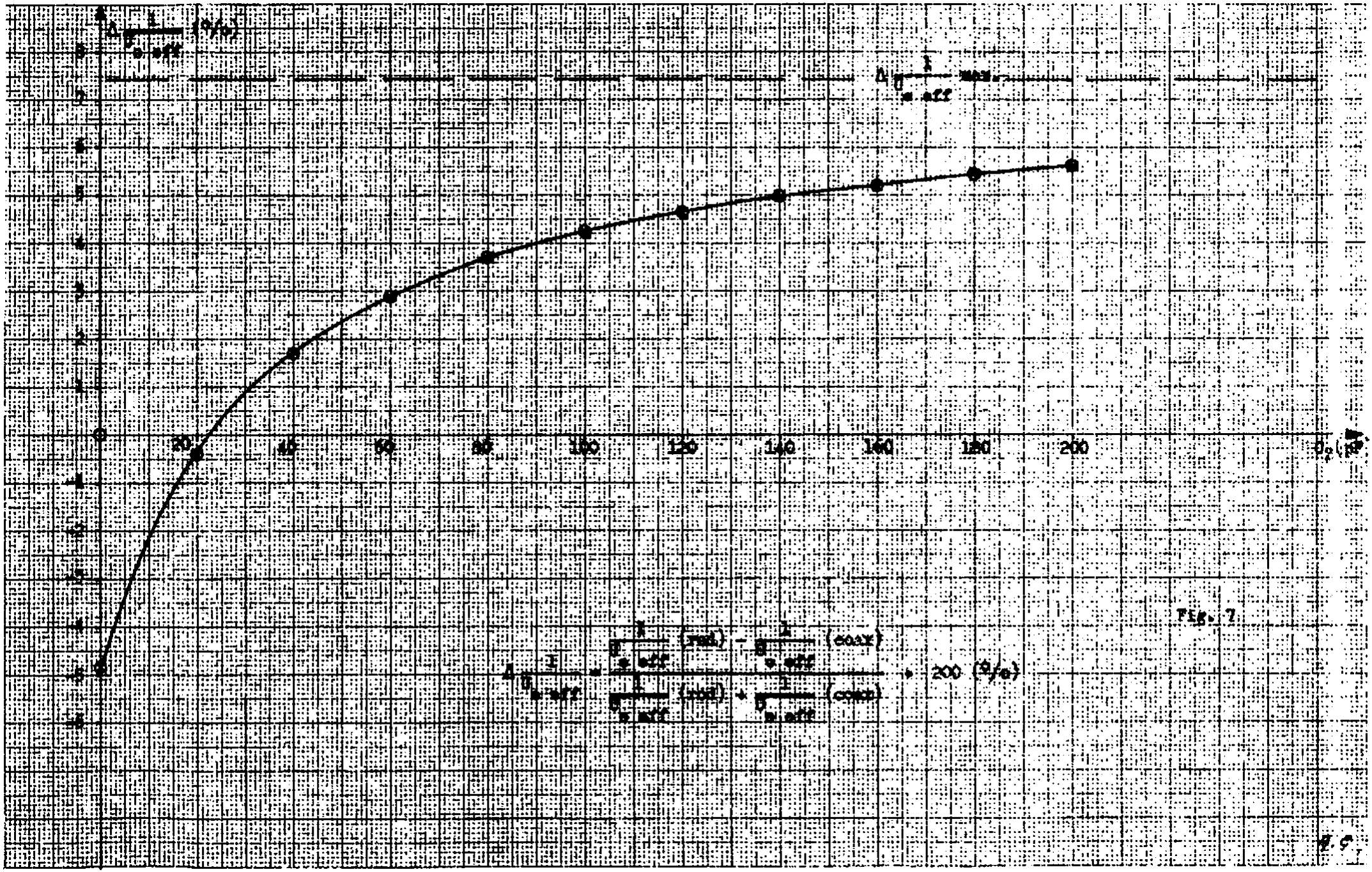
$\Delta \frac{1}{Q_{a\,eff}}$ (%)
$\Delta \frac{1}{Q_{a\,eff}}$ max.
20
40
60
80
100
120
140
160
180
200
θ_c (mm)
$\Delta \frac{1}{Q_{a\,eff}} = \frac{\frac{1}{Q_{a\,eff}}(rect) - \frac{1}{Q_{a\,eff}}(coax)}{\frac{1}{Q_{a\,eff}}(rect) + \frac{1}{Q_{a\,eff}}(coax)} \cdot 200$ (%)

Fig. 7

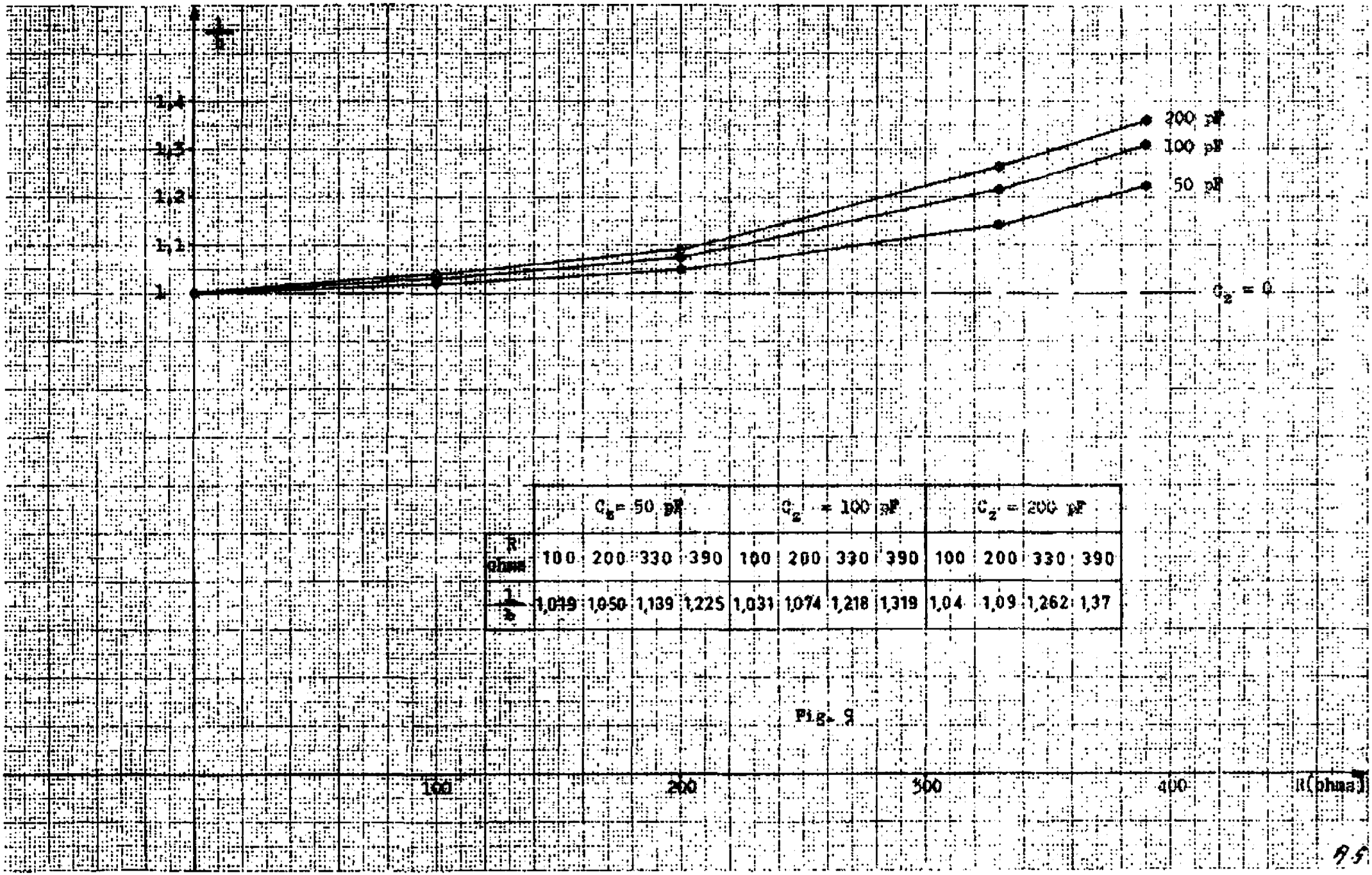

	C_2 = 50 pF				C_2 = 100 pF				C_2 = 200 pF			
R ohms	100	200	330	390	100	200	330	390	100	200	330	390
$\frac{1}{b}$	1,019	1,050	1,139	1,225	1,031	1,074	1,218	1,319	1,04	1,09	1,262	1,37

Fig. 9

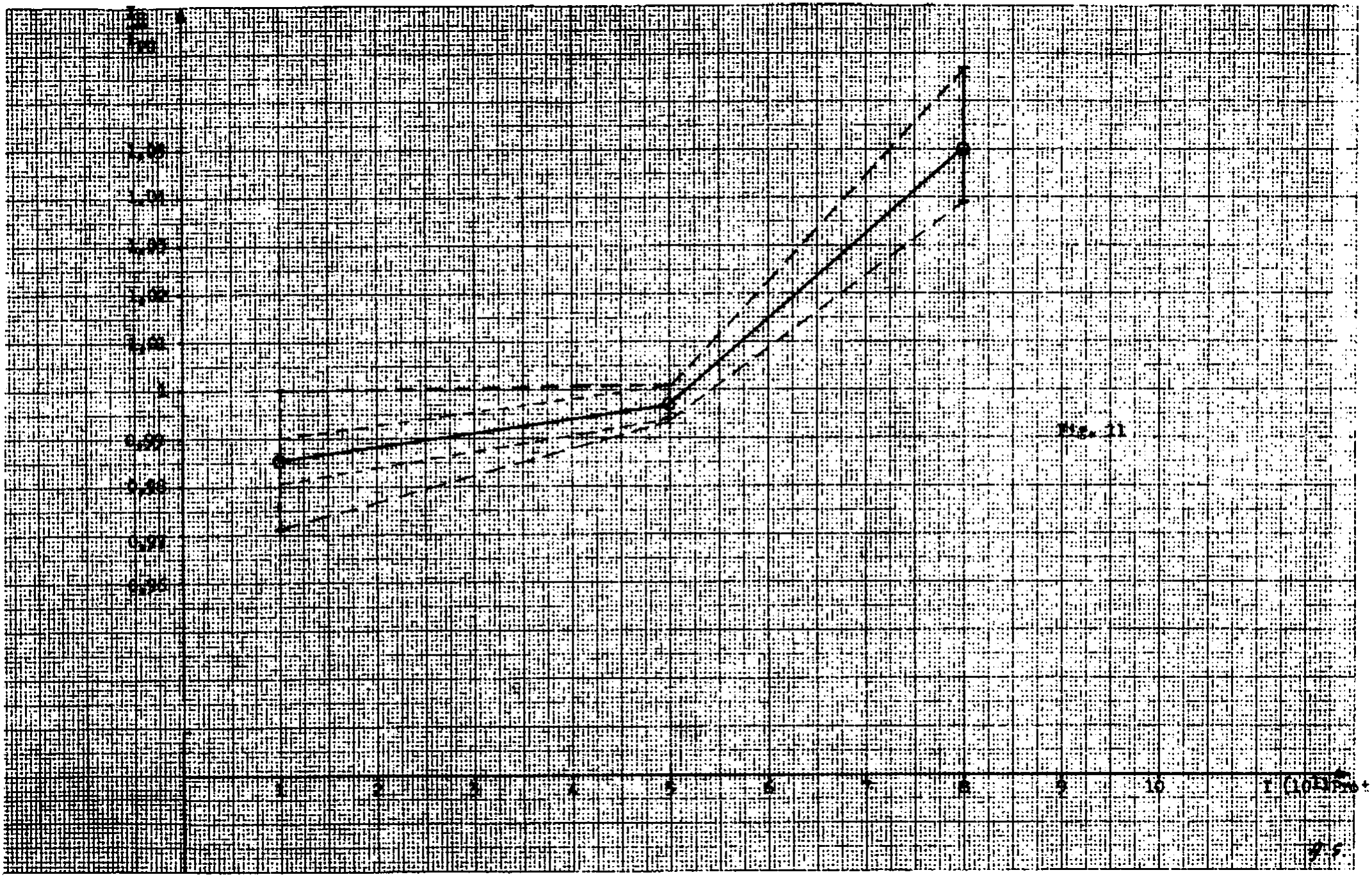
1
2
3
4
5
6
7
8
9
10
Fig. 11

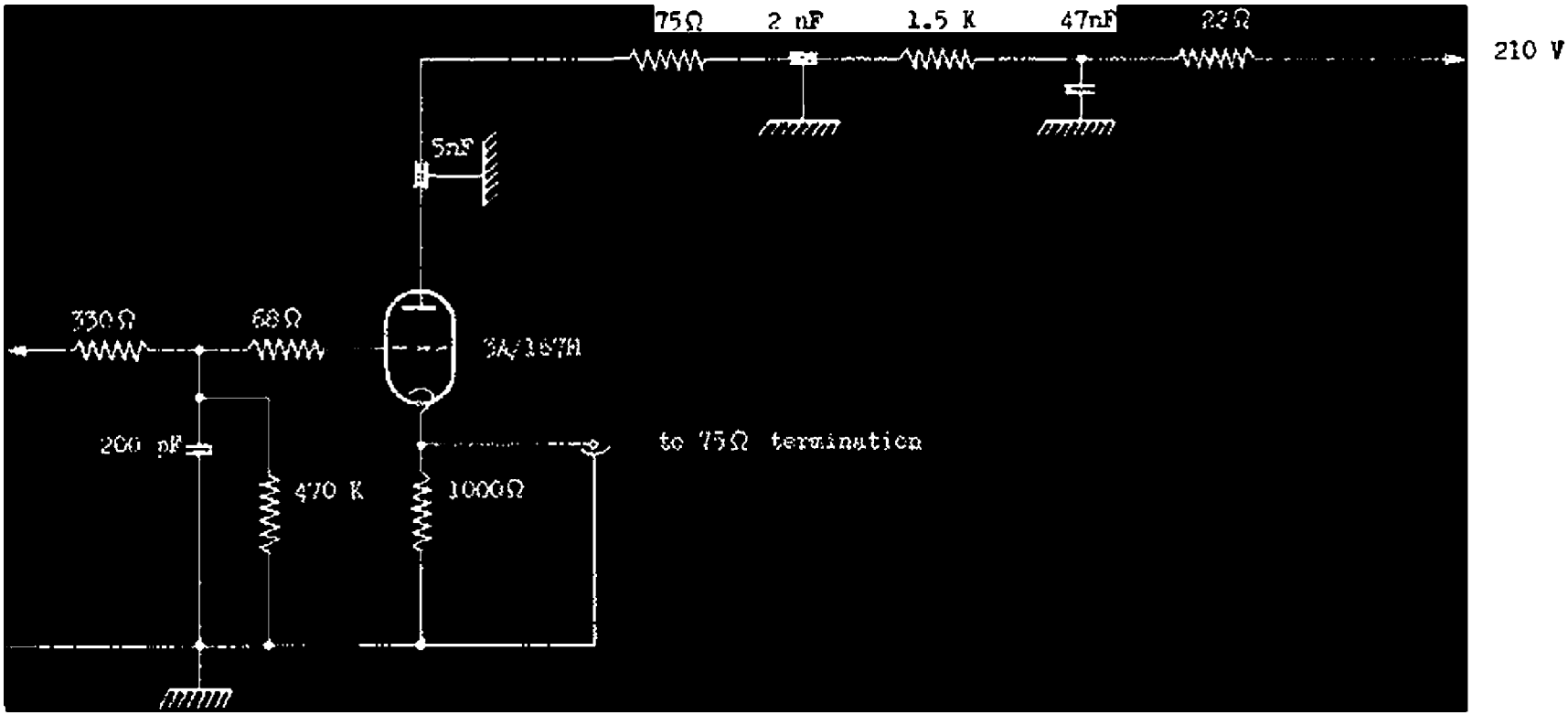
75Ω
2 nF
1.5 K
47nF
22Ω
210 V
5nF
330Ω
68Ω
3A/157A
200 pF
470 K
1000Ω
to 75Ω termination

Fig. 14

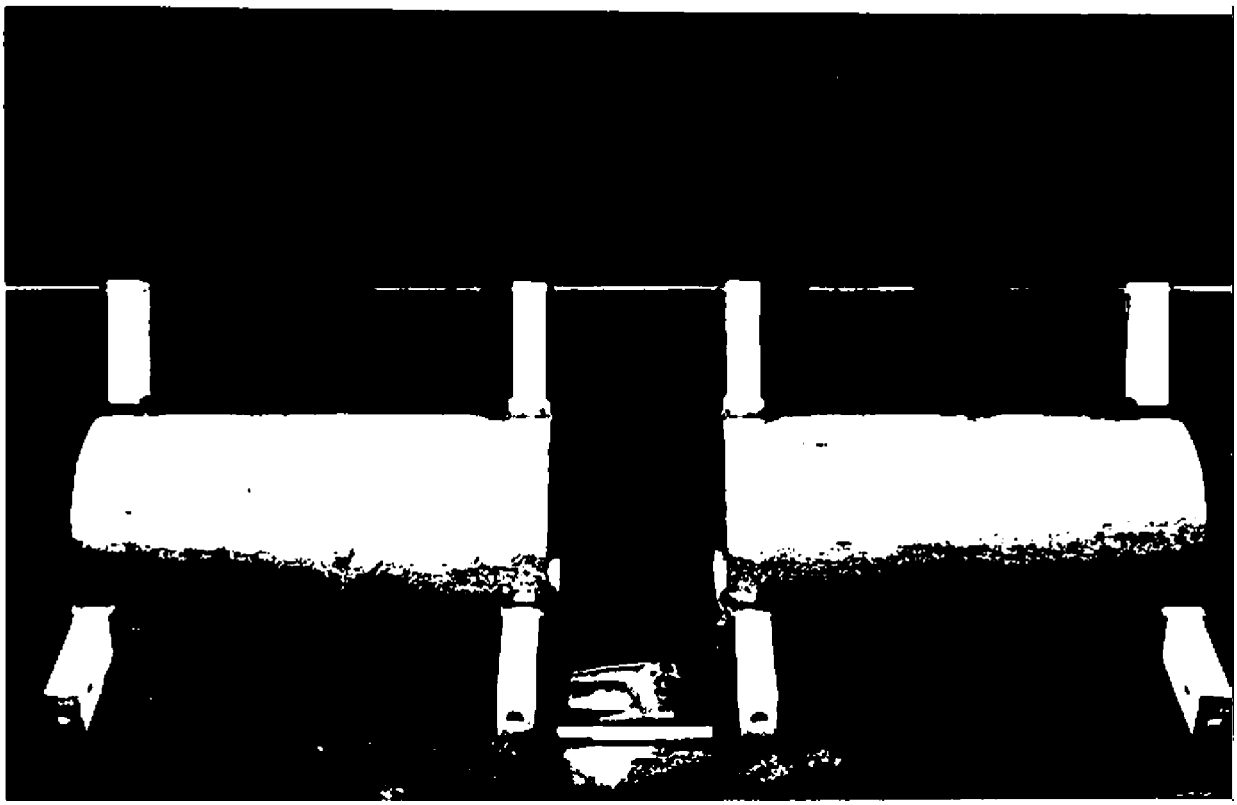

Photo no. 1

The electrodes of the PU station with centre conductor

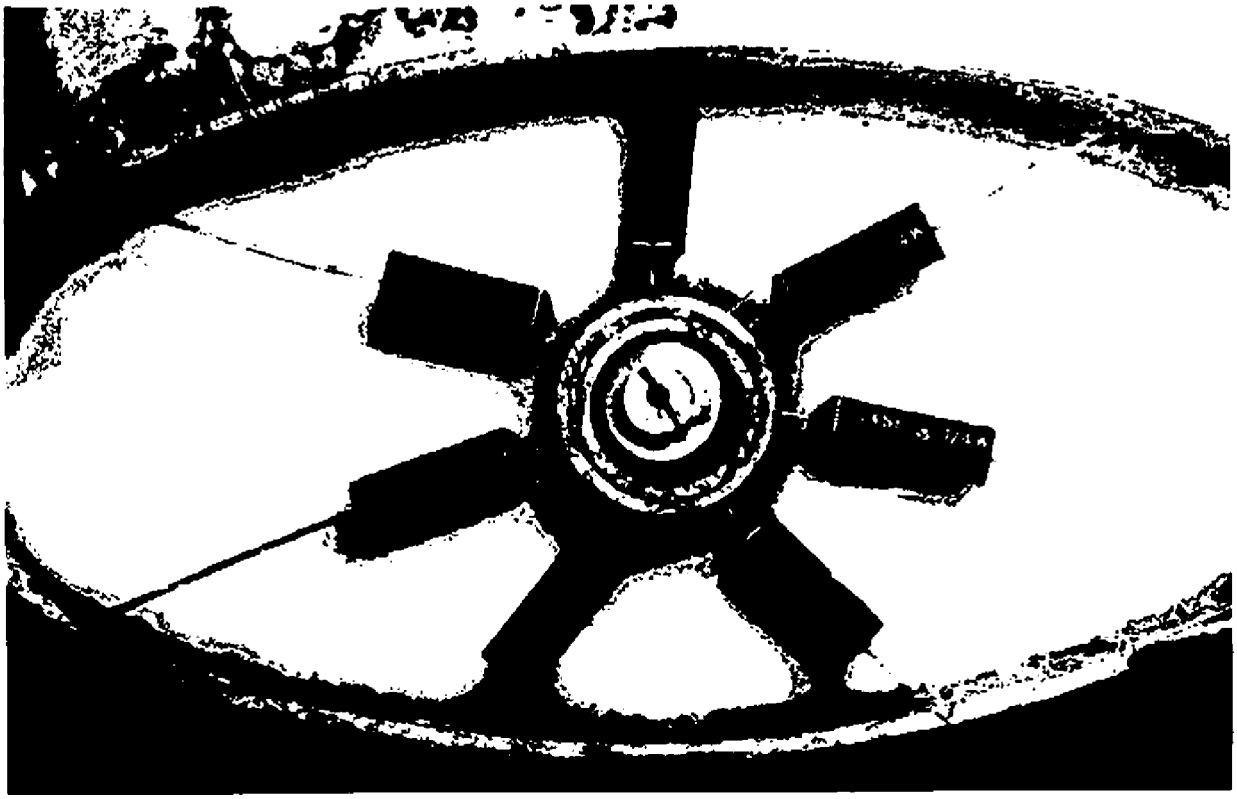

Photo no. 2

Terminal resistance

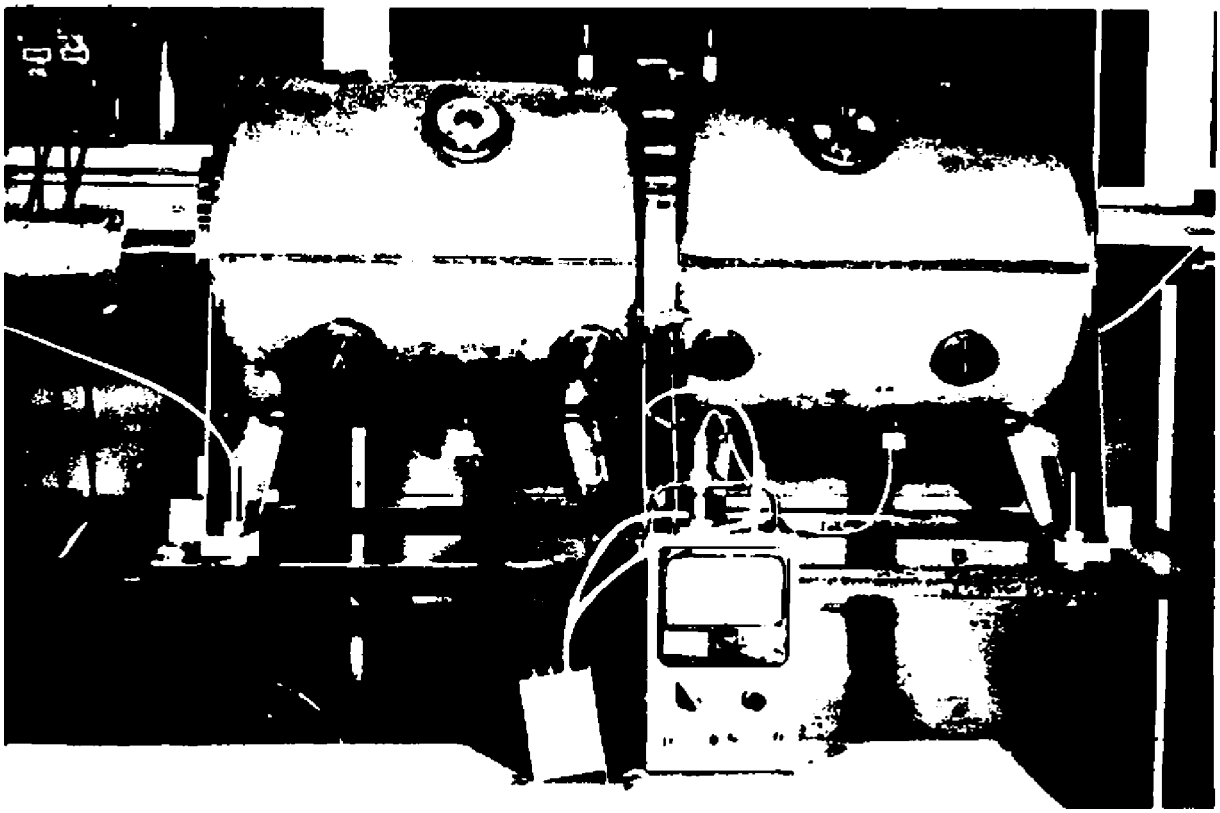

Photo no. 3

Measuring arrangement for charged rod measurements

Photo no. 4

Test electrode with rod

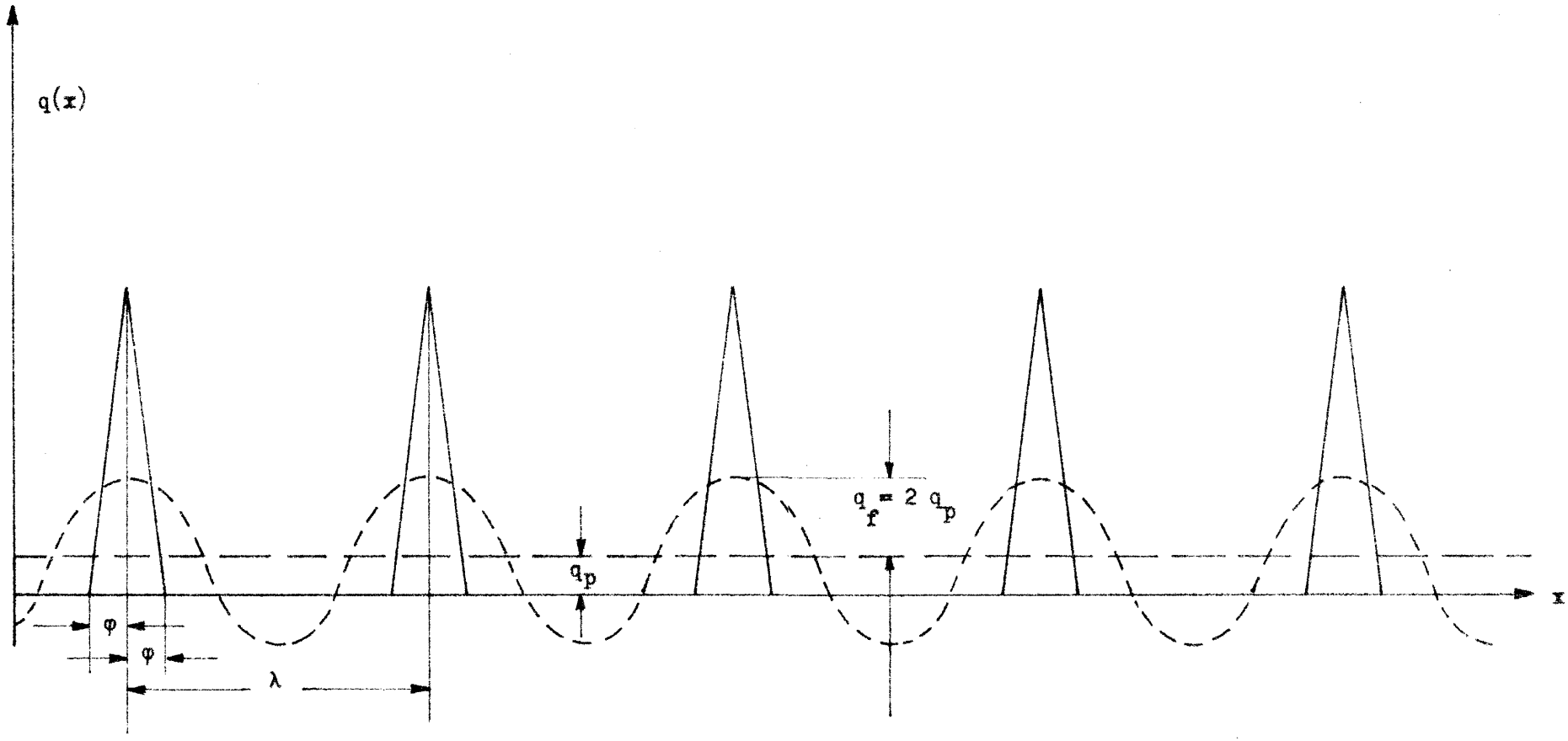

Fig. 1

A. S.

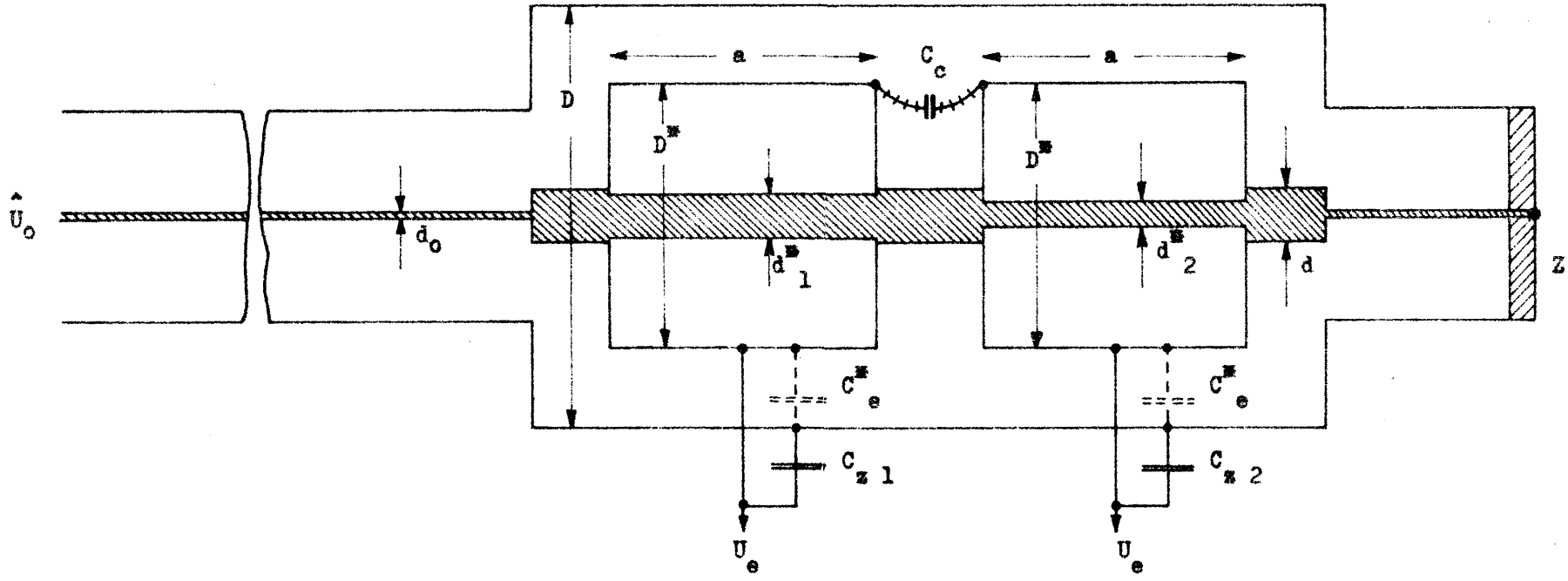

Fig. 2

A.S.

$\frac{1}{U_{e\ eff}}$ $(\frac{1}{V})$

C_{el} = 36,5 pF; $tg\,\alpha_1 = 0{,}0784 \cdot 10^{12}\ (\frac{1}{F;\ V_{eff}})$; $A_p = 10^{11}$

α_1

Fig. 3

P.S.

SIS/R/7983

C_x [pF]

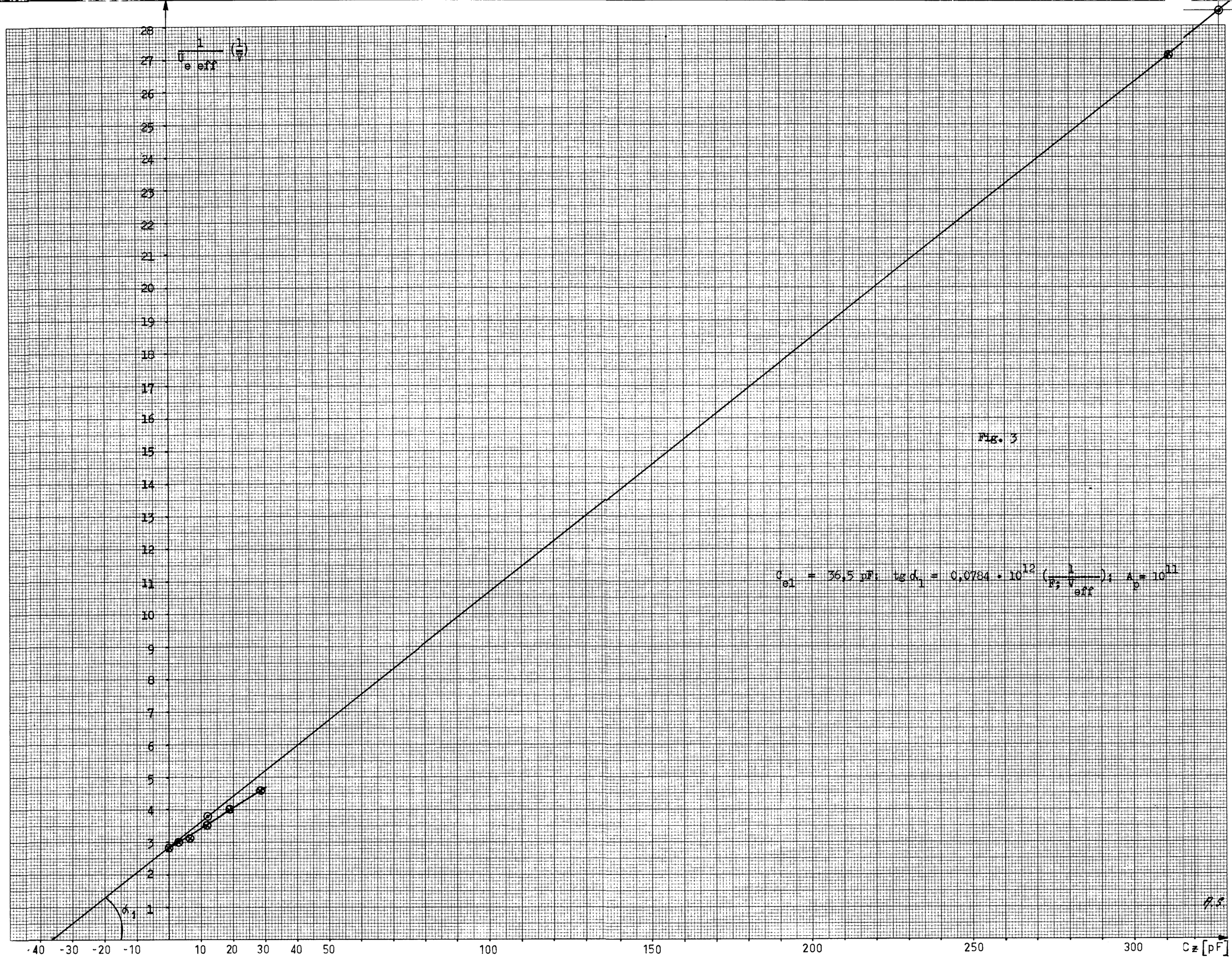

Fig. 3

P.S.

SIS/K/7983

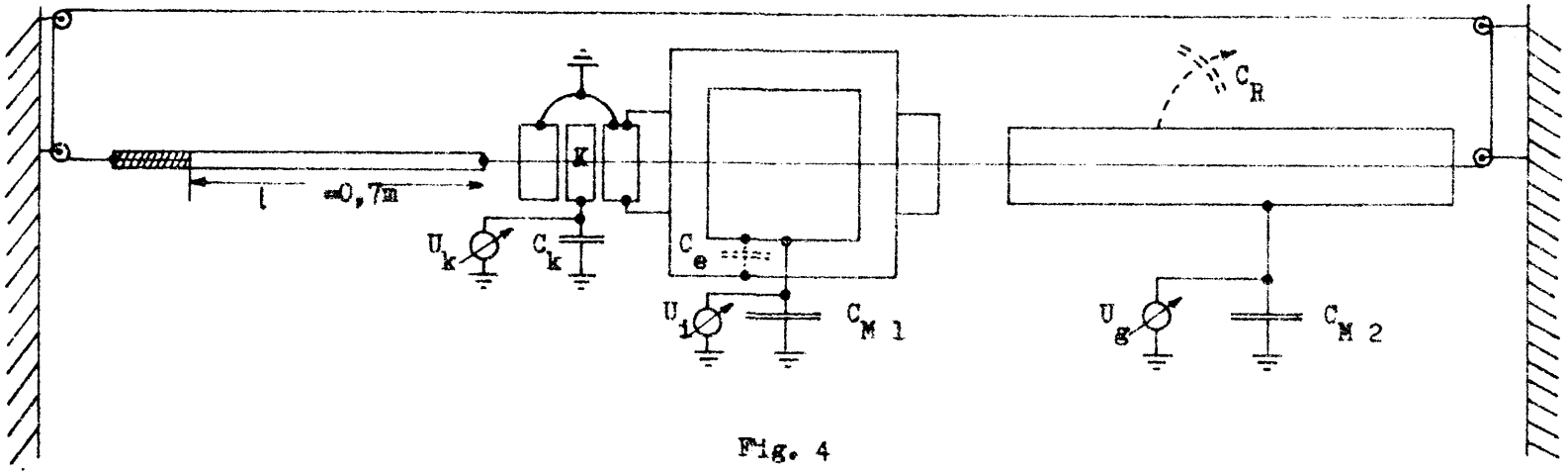

Fig. 4

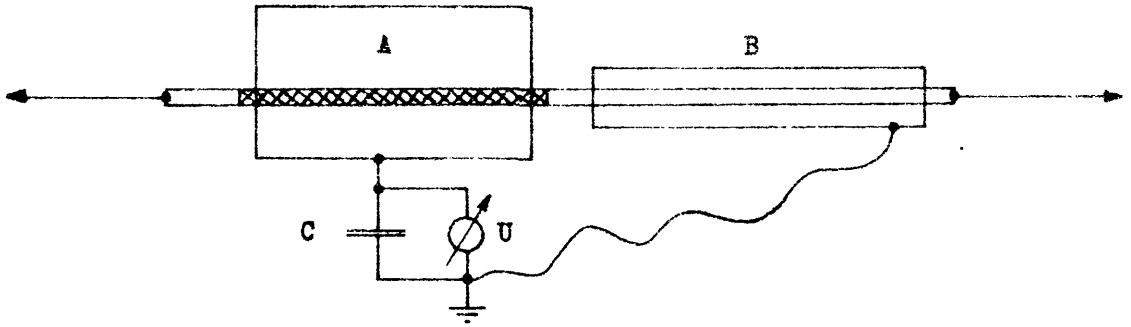

Fig. 5

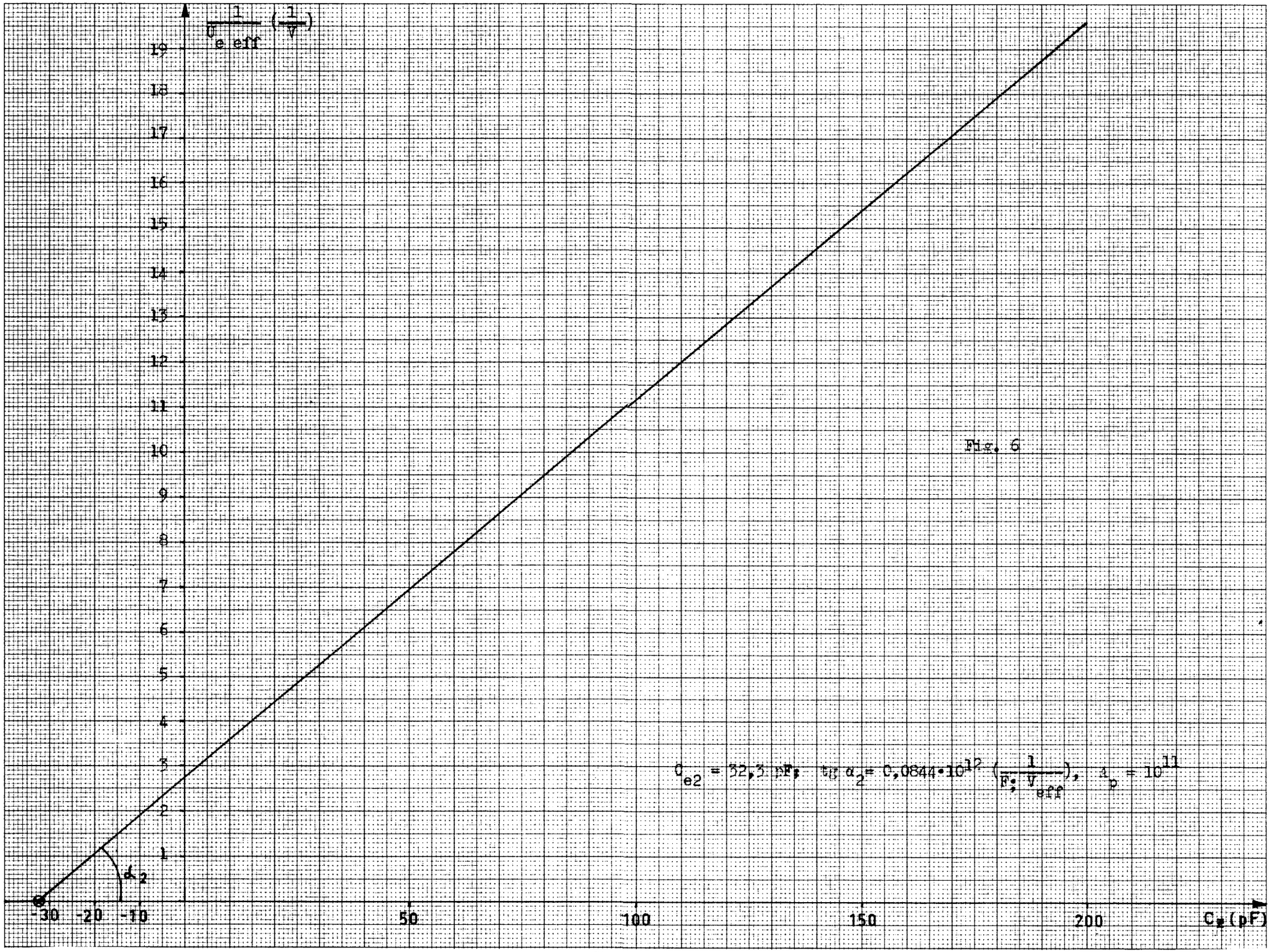

Fig. 6

$C_{e2} = 32{,}3$ pF; tg $\alpha_2 = 0{,}0844 \cdot 10^{12}$ $(\frac{1}{F; \frac{1}{V_{eff}}})$, $A_p = 10^{11}$

$\frac{1}{U_{e\,eff}}$

R = 390 Ω

R = 330 Ω

R = 200 Ω

R = 100 Ω

R = 0

Fig. 10

$C_e' = C_e + C_{z0} = 32{,}3 + 8 \approx 40$ pF

C_z [pF]

$A_p \cdot 10^{-11}$ (R = 330 ohms; C = 200 pF)

10
9
8
7
6
5
4
3
2
1
0,5

theoretical
measured

20 30 40 50 60 70 80 90 100 150 200 250 300 350 400

U_g (mV)

Transfer function from grid cathode-follower to digital indication.
Calibration at $5 \cdot 10^{11}$ protons.

Fig. 12

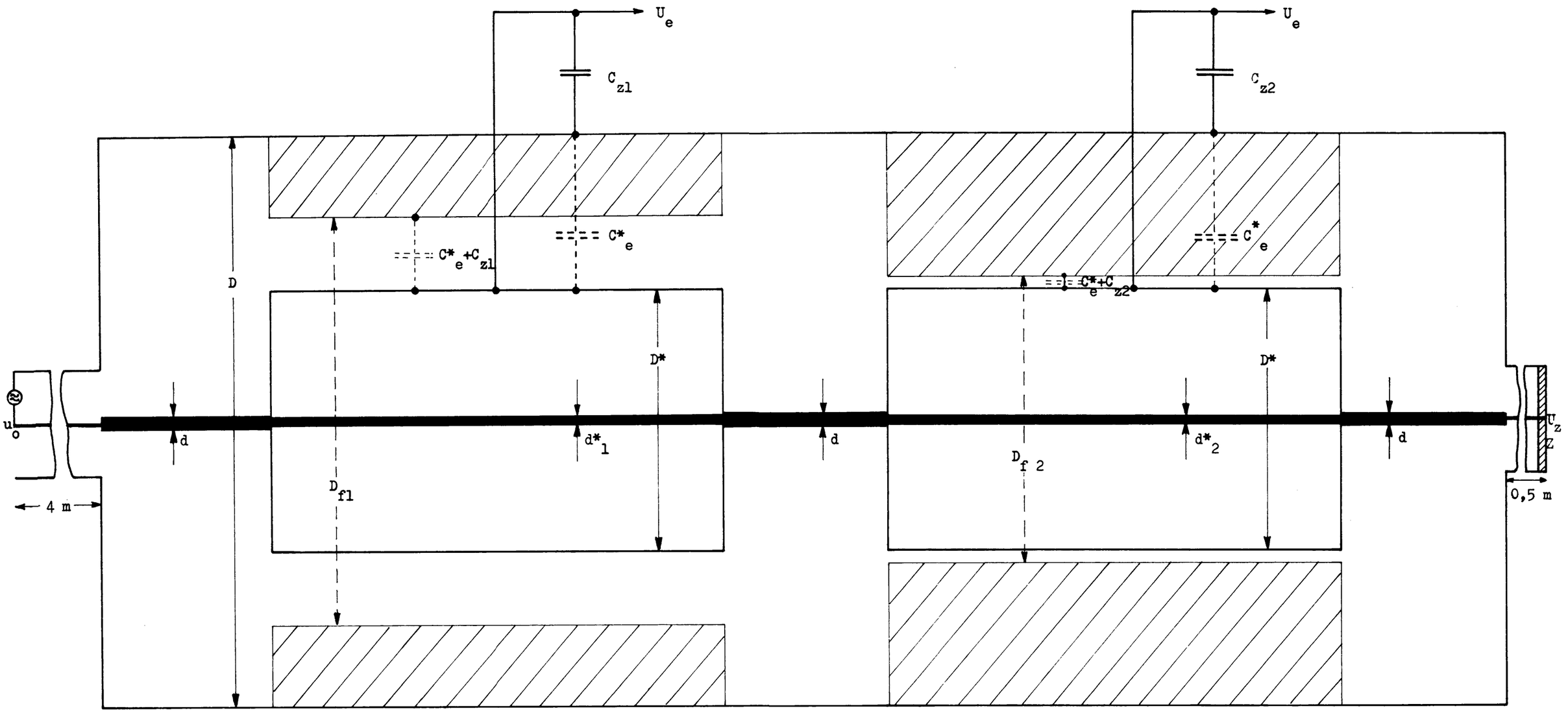
U_e
C_z1
C*_e+C_z1
C*_e
D
D*
d
d*_1
D_f1
4 m
u_o
U_e
C_z2
C*_e
C*_e+C_z2
D*
d
d*_2
D_f 2
d
U_z
Z
0,5 m

Fig. 13